JACS
JOURNAL OF THE AMERICAN CHEMICAL SOCIETY

Subscriber access provided by American Chemical Society

Article

Utilization of a Combination of Weak Hydrogen-Bonding Interactions and Phase Segregation to Yield Highly Thermosensitive Supramolecular Polymers

Sona Sivakova, David A. Bohnsack, Michael E. Mackay, Phiriyatorn Suwanmala, and Stuart J. Rowan

J. Am. Chem. Soc., **2005**, 127 (51), 18202-18211• DOI: 10.1021/ja055245w • Publication Date (Web): 30 November 2005

Downloaded from http://pubs.acs.org on March 25, 2009

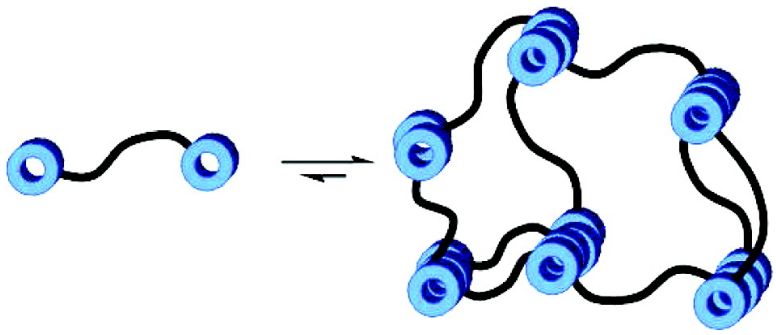

More About This Article

Additional resources and features associated with this article are available within the HTML version:

- Supporting Information
- Links to the 24 articles that cite this article, as of the time of this article download
- Access to high resolution figures
- Links to articles and content related to this article
- Copyright permission to reproduce figures and/or text from this article

View the Full Text HTML

ACS Publications
High quality. High impact.

Journal of the American Chemical Society is published by the American Chemical Society. 1155 Sixteenth Street N.W., Washington, DC 20036

J|A|C|S
ARTICLES
Published on Web 11/30/2005

Utilization of a Combination of Weak Hydrogen-Bonding Interactions and Phase Segregation to Yield Highly Thermosensitive Supramolecular Polymers

Sona Sivakova,[†] David A. Bohnsack,[‡] Michael E. Mackay,*[,‡] Phiriyatorn Suwanmala,[†] and Stuart J. Rowan*[,†]

Contribution from the Department of Macromolecular Science and Engineering, Case Western Reserve University, 2100 Adelbert Road, Cleveland, Ohio 44106-7202, and Department of Chemical Engineering and Materials Science, Michigan State University, East Lansing, Michigan 48824

Received August 2, 2005; E-mail: stuart.rowan@case.edu; mackay@egr.msu.edu.

Abstract: Supramolecular polymerization, i.e., the self-assembly of polymer-like materials through the utilization of the noncovalent bond, is a developing area of research. In this paper, we report the synthesis and investigation of nucleobase-terminated (N^6-anisoyl-adenine and N^4-(4-*tert*-butylbenzoyl)cytosine) low molecular weight poly(THF) macromonomers (<2000 g mol^{-1}). Even though the degree of interaction between the nucleobase derivatives is very low (<5 M^{-1}) these macromonomers self-assemble in the solid state to yield materials with film and fiber-forming capability. While the mechanical properties of films of both materials show extreme temperature sensitivity, resulting in the formation of very low viscosity melts, they do behave differently, which is attributed to the nature of the self-assembly controlled by the nucleobase. A combination of FT-IR, WAXD, and rheological experiments was carried out to further investigate the nature of the self-assembly in these systems. The studies demonstrate that a combination of phase segregation between the hard nucleobase chain ends and the soft poly(THF) core combined with aromatic amide hydrogen bonding is utilized to yield the highly thermosensitive supramolecular polymeric materials. In addition, analysis of the data suggests that the rheological properties of these supramolecular materials is controlled by the disengagement rate of the nucleobase chain ends from the "hard" phase, which, if shown to be general, provides a design criteria in the development of more thermally responsive materials.

Introduction

In recent years, the field of supramolecular polymers, and in particular supramolecular polymerizations, has seen a dramatic growth in activity.[1] A number of groups have investigated the use of noncovalent interactions to organize monomers into larger supramolecular polymeric aggregates, in which the polymer consists of noncovalent as well as covalent bonds (e.g., Figure 1a). The result is, therefore, materials which exhibit a number of interesting and unusual properties: (1) they form spontaneously, without the need for an initiation process or catalyst; (2) termination processes during the polymerization (self-assembly) are limited; (3) they are "dynamic", i.e., they are formed under reversible conditions. The consequence of such behavior is that the degree of polymerization (DP) depends, to a large extent, on the strength of the supramolecular interaction between the monomers as well as the monomer concentration. Anything that affects the strength of the binding constant and/or the monomer concentration will drastically affect the DP of the material, and consequently, the properties of these "dynamic" polymers should be very sensitive to environmental conditions. Thus, the development of materials self-assembled through a supramolecular polymerization process opens the door to systems that are extremely thermally responsive and exhibit low melt viscosities. Such polymers offer facile processing or recycling and have potential as thermally re-healable materials.[2,3]

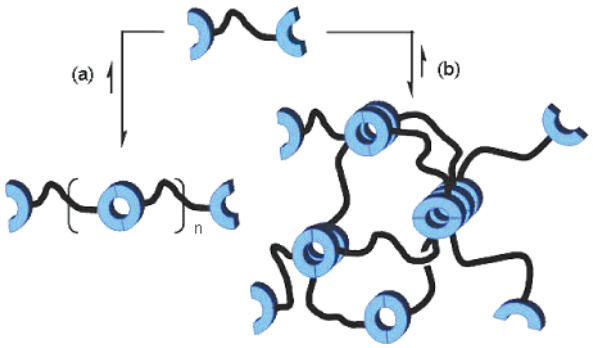

Figure 1. Schematic representation of (a) a linear supramolecular polymer and (b) the use of phase segregation to construct a supramolecular network in the solid state.

[†] Case Western Reserve University.
[‡] Michigan State University.

(1) (a) Brunsveld, L.; Folmer, B. J. B.; Meijer, E. W.; Sijbesma, R. P. *Chem. Rev.* **2001**, *101*, 4071−4097. (b) Ciferri, A. *Macromol. Rapid Commun.* **2002**, *23*, 511−529. (c) *Supramolecular Polymers*, 2nd ed.; Ciferri, A., Ed.; CRC Press: Taylor and Francis: Boca Raton, FL, 2005.

(2) For a recent example of a thermally rehealable polymer which utilized reversible covalent bonds, see: Chen, X.; Dam, M. A.; Ono, K.; Mal, A.; Shen, H.; Nut, S. R.; Sheran, K.; Wudl, F. *Science* **2002**, *295*, 1698−1702.

10.1021/ja055245w CCC: $30.25 **© 2005 American Chemical Society**

If growth of such a supramolecular polymer[4] operates through a *multistage open association mechanism* (*MSOA*), which is essentially a reversible step-growth process where the binding constant is independent of the molecular weight (i.e., no cooperation) and assuming no ring formation, then the DP will be approximately proportional to $(K_a[M])^{1/2}$, where K_a is the binding constant and [M] is the total concentration of monomers. As such, large values of K_a are generally required to obtain aggregates of significant molecular weight in dilute solutions. This has led to the development of a range of supramolecular motifs which exhibit large binding constants ($>10^6$ M^{-1}).[5] In particular, a number of different hydrogen-bonding motifs and metal/ligand motifs have been developed and successfully utilized in the preparation of supramolecular materials.[6,7] One of the most elegant and successfully employed motifs for supramolecular polymerizations is the quadruple hydrogen-bonding ureidopyrimidone developed by Sijbesma, Meijer, and co-workers which has a dimerization constant of about 10^7 M^{-1} in chloroform.[8] Attachment of this motif to the chain ends of a macromonomer results in enhancement of polymer properties in both solution and solid state.[6a,9] It should be noted here that in many of these systems phase segregation has been shown to occur between the strongly interacting end group and polymeric core.

While the use of strongly binding supramolecular motifs has proved very successful, there are a number of possible drawbacks associated with this approach when aimed at the development of thermally responsive polymers in the solid state. The first issue deals with the thermodynamic stability of such strongly interacting monomers which may require high temperatures to significantly depolymerize the resulting polymeric aggregate. If weaker binding motifs can be utilized then potentially lower depolymerization temperatures (akin to ceiling temperature) could be used. The second issue is more concerned with the kinetic stability of the system where, in general, the rates for complexation/decomplexation decrease as the strength of the binding constant increases, which in turn potentially reduces the responsiveness of the material. Furthermore, there is a limited number of very strongly interacting binding motifs currently available. Thus, with the goal of generating supramolecular materials which exhibit a highly sensitive thermal response in the solid state, we set out to investigate the potential of utilizing telechelic compounds in which the self-assembly of the macromonomer species is controlled by weakly binding, labile hydrogen-bonding motifs. Such materials should then exhibit a range of unusual polymer-like properties, including very low melt and solution viscosities along with high-temperature sensitivity in the bulk state. If this could be achieved then it would also suggest a much wider range of noncovalent motifs which could be utilized in supramolecular polymerizations.

To realize such materials, other noncovalent interactions and ordering effects must be used in addition to the weak hydrogen bonding. This is not without precedent as, for example, liquid crystalline ordering has successfully lead to supramolecular polymers from monomers which contain weak hydrogen-bonding units.[10,11] Furthermore, with the increased interest in the supramolecular chemistry of block copolymers,[12] phase segregation has become a powerful tool to control solid-state morphology and properties. Such work has led to ABA triblock copolymers being used in many aspects of the polymer industry from foams to emulsions to fibers.[13] In general, these materials phase separate into soft and hard blocks where the end groups usually constitute the hard block to create a robust network.

We rationalized that we may be able to achieve significant polymer-like properties with low molecular weight compounds in which a soft core segment has weakly interacting hydrogen-bonding hard segments attached at either end (Figure 1b). If phase segregation occurs then this should enhance the degree of interaction of the end groups by increasing their effective molarity.[14] Additionally, the presence of the hydrogen bonding may aid phase segregation. There are a few examples in the literature where hydrogen bonding combined with phase segregation has been investigated. Stadler and co-workers,[15,16]

(3) For an example of a self-healing material which operates using a different mechanism, see: White, S. R.; Sottos, N. R.; Geubelle, P. H.; Moore, J. S.; Kessler, M. R.; Sriram, S. R.; Brown, E. N.; Viswanathan, S. *Nature* **2001**, *409*, 794−797.

(4) Ciferri, A. Growth of Supramolecular Structures. In *Supramolecular Polymers*, 2nd ed.; Ciferri, A., Ed.; CRC Press: Taylor and Francis: Boca Raton, FL, 2005; Chapter 2.

(5) (a) Corbin, P. S.; Zimmerman, S. C. *J. Am. Chem. Soc.* **1998**, *120*, 9710−9711. (b) Corbin, P. S.; Zimmerman, S. C. *J. Am. Chem. Soc.* **2000**, *122*, 3779−3780. (c) Mayer, M. F.; Nakashima, S.; Zimmerman S. C. *Org. Lett.* **2005**, *7*, 3005−3008. (d) Zeng, H.; Yang, X.; Brown, A. L.; Martinovic, S.; Smith, R. D.; Gong, B. *Chem. Commun.* **2003**, 1556−1557.

(6) (a) Sijbesma, R. P.; Beijer, F. H.; Brunsveld, L.; Folmer, B. J. B.; Hirschberg, J. H. K. K.; Lange, R. F. M.; Lowe, J. K. L.; Meijer, E. W. *Science* **1997**, *278*, 1601−1604. (b) Castellano, R. K.; Rudkevich, D. M.; Rebek, J., Jr. *Proc. Natl. Acad. Sci. U.S.A.* **1997**, *94*, 7132−7137. (c) Vollmer, M. S.; Clark, T. D.; Steinem, C.; Ghadiri, M. R. *Angew. Chem., Int. Ed.* **1999**, *38*, 1598−1601. (d) Zimmerman, S. C.; Zeng, F. W.; Reichert, D. E. C.; Kolotuchin, S. V. *Science* **1996**, *271*, 1095−1098. (e) Yang, X.; Hua, F.; Yamato, K.; Ruckenstein, E.; Gong, B.; Kim, W.; Ryu, C. Y. *Angew. Chem., Int. Ed.* **2004**, *43*, 6471−6474. (f) Hua, F.; Yang, X.; Gong, B.; Ruckenstein, E. *J. Polym. Sci., Part A: Polym. Chem.* **2005**, *43*, 1119−1128. (g) Ligthart, G. B. W. L.; Ohkawa, H.; Sijbesma, R. P.; Meijer, E. W. *J. Am. Chem. Soc.* **2005**, *127*, 810−811. (h) Park, T.; Zimmerman, S. C.; Nakashima, S. *J. Am. Chem. Soc.* **2005**, *127*, 6520−6521.

(7) (a) Hinderberger, D.; Schmelz, O.; Rehahn, M.; Jeschke, G. *Angew. Chem., Int. Ed.* **2004**, *43*, 4616−4621. (b) Schmatloch, S.; van den Berg, A. M. J.; Alexeev, A. S.; Hofmeier, H.; Schubert, U. S. *Macromolecules* **2003**, *36*, 9943−9949. (c) Dobrawa, R.; Lysetska, M.; Ballester, P.; Grüne, M.; Würthner, F. *Macromolecules* **2005**, *38*, 1315−1325. (d) Kurth, D. G.; Meister, A.; Thuenemann, A. F.; Foerster, G. *Langmuir* **2003**, *19*, 4055−4057. (e) Vermonden, T.; van Steenbergen, M. J.; Besseling, N. A. M.; Marcelis, A. T. M.; Hennink, W. E.; Sudhoelter, E. J. R.; Cohen Stuart, M. A. *J. Am. Chem. Soc.* **2004**, *126*, 15802−15808. (f) Yount, W. C.; Juwarker, H.; Craig, S. L. *J. Am. Chem. Soc.* **2003**, *125*, 15302−15303. (g) Paulusse, J. M. J.; Sijbesma, R. P. *Angew. Chem., Int. Ed.* **2004**, *43*, 4460−4462. (h) Beck, J. B.; Rowan, S. J. *J. Am. Chem. Soc.* **2003**, *125*, 13922−13923. (i) Colombani, O.; Baroiz, C.; Bouteiller, L.; Chanéac, C.; Frompérie, L.; Lortie, F.; Montès, H. *Macromolecules* **2005**, *38*, 1752−1759.

(8) (a) Beijer, F. H.; Sijbesma, R. P.; Kooijman, H.; Spek, A. L.; Meijer, E. W. *J. Am. Chem. Soc.* **1998**, *120*, 6761−6769. (b) Söntjens, S. H. M.; Sijbesma, R. P.; van Genderen, M. H. P.; Meijer, E. W. *J. Am. Chem. Soc.* **2000**, *122*, 7487−7493.

(9) Folmer, B. J. B.; Sijbesma, R. P.; Versteegen, R. M.; van der Rijt, J. A. J.; Meijer, E. W. *Adv. Mater.* **2000**, *12*, 874−878.

(10) (a) Lehn, J.-M. *Polym. Int.* **2002**, *51*, 825−839. (b) Kato, T.; Mizoshita, N.; Kanie, K. *Macromol. Rapid Commun.* **2001**, *22*, 797−814. (c) Paleos, C. M.; Tsiourvas, D. *Liq. Cryst.* **2001**, *28*, 1127−1161. (d) Ciferri, A. *Liq. Cryst.* **1999**, *26*, 489−494.

(11) (a) Gulik-Krzywicki, T.; Fouquey, C.; Lehn, J.-M. *Proc. Natl. Acad. Sci. U.S.A.*, **1993**, *90*, 163−167. (b) Bladon, P.; Griffin, A. C. *Macromolecules* **1993**, *26*, 6604−6610. (c) Kotera, M.; Lehn, J.-M.; Vigneron, J.-P. *J. Chem. Soc., Chem. Commun.* **1994**, *2*, 197−199. (d) Kotera, M.; Lehn, J.-M.; Vigneron, J.-P. *Tetrahedron* **1995**, *51*, 1953−1972. (e) St. Pourcain, C.; Griffin, A. C. *Macromolecules* **1995**, *28*, 4116−4121.

(12) For some recent reviews, see: (a) Ruzette, A.-V.; Leibler, L. *Nat. Mater.* **2005**, *4*, 19−31. (b) Lee, M.; Cho, B.-K.; Zin, W.-C. *Chem. Rev.* **2001**, *101*, 3869−3892. (c) Klok, H.-A.; Lecommandoux, S. *Adv. Mater.* **2001**, *13*, 1217−1229. (d) Stupp, S. I. *Curr. Opin. Colloid Interface Sci.* **1998**, *3*, 20−26. (e) Foerster, S.; Antonietti, M. *Adv. Mater.* **1998**, *10*, 195−217.

(13) Bates, F. S.; Fredrickson, G. H. *Phys. Today* **1999**, *52* (2), 32−38.

(14) Kirby, A. J. *Adv. Phys. Org. Chem.* **1980**, *17*, 183−278.

(15) Müller, M.; Dardin, A.; Seidel, U.; Balsamo, V.; Iván, B.; Spiess, H. W.; Stadler, R. *Macromolecules* **1996**, *29*, 2577−2583.

(16) For related polymers in which the hydrogen-bonding units are attached as side chains, see for example: (a) Hilger, C.; Stadler, R.; De Lucca, F.; Liane, L. *Polymer* **1990**, *31*, 818−23. (b) Hilger, C.; Stadler, R. *Macromolecules* **1992**, *25*, 6670−6680. (c) Hilger, C.; Dräger, M.; Stadler, R. *Macromolecules* **1992**, *25*, 6670−6680.

Lillya et al.[17] and, more recently, Duweltz et al.[18] have investigated low-T_g polymers in which hydrogen-bonding groups, in the form of either 4-urazoyl benzoic acid or benzoic acid derivatives, are attached to either end of the chain. In these systems the end groups crystallize or phase segregate to form the physical cross-links which results in an enhancement of mechanical properties.

The goal of the present work is to examine this phase-segregation-aided supramolecular polymerization approach in more detail and investigate the potential of other weak hydrogen-bonding groups. Thus we decided to investigate simple nucleobase derivatives as the self-assembly units.[19] Utilization of the common nucleobases as the binding motif in supramolecular assemblies[20] offers the flexibility of exploiting four different binding units—adenine (A), cytosine (C), guanine (G), and thymine (T)—all of which offer different binding characteristics. These groups serve as a test bed for comparing the effects of end group selection on the materials' self-assembly and resulting mechanical properties. In addition to the complementary interactions, all of the nucleobases can homoaggregate, albeit with greatly reduced binding constants ($K_{TT} = 3.5\ M^{-1}$, $K_{AA} = 2.4\ M^{-1}$, $K_{CC} = 40\ M^{-1}$, $K_{GG} = 10^2$ to $10^4\ M^{-1}$ in $CDCl_3$).[21] Therefore, monomer units which contain single nucleobase binding sites should exhibit degrees of hydrogen bonding too low to form polymers through the *MSOA mechanism* in solution.

So rather than use underivatized nucleobases we have chosen to focus our attention on aromatic amide protected nucleobases. This was done for two reasons; the first was to reduce the type and amount of hydrogen bonding possible with the nucleobases. While DNA sequences are one of the most predictable supramolecular binding motifs,[22] the individual nucleobases are less well behaved. For example, the purines (adenine and guanine) are able to bind through two different binding sites (Watson−Crick and Hoogsteen),[23,24] and as a result can form multicomponent complexes. The second reason was to increase the size of the hard nucleobase segment and as such encourage the phase segregation[25−28] of the "soft" poly(THF) core[17,29] and "hard" nucleobase chain ends. Furthermore, some of us have previously shown that a bis-N^6-anisoyl-adenine ($\mathbf{A^{An}}$) functionalized monomer can be used in conjunction with a bis-thymine monomer to form liquid crystalline supramolecular polymers.[30]

Scheme 1. Synthetic Procedure Used to Obtain the Ditopic Macromonomers

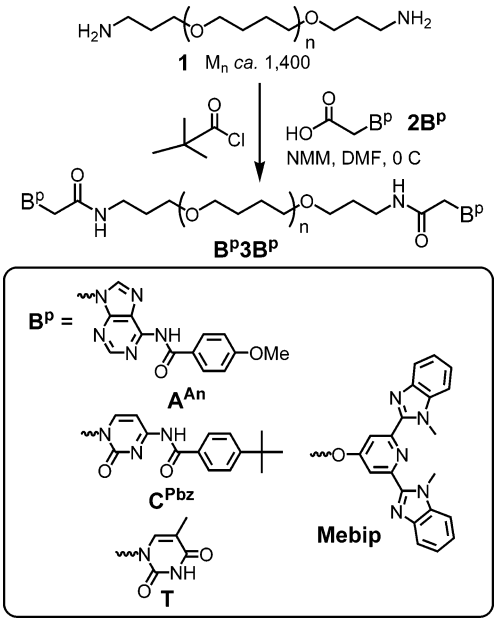

Results and Discussion

Synthesis of the Nucleobase End-Functionalized Macromonomers. The nature of the core unit that is placed between the nucleobases will play an important role in the resulting material's mechanical, functional, and even self-assembly properties. In this work we have focused on commercially available low molecular weight bis(3-aminopropyl)-terminated polytetrahydrofuran, **1** (M_n ca. 1400 g mol^{-1}), as the macromonomer core. We chose this core on account of the low glass transition temperature ($T_g = -86$ °C) of poly(THF). We have previously shown that the end capping of **1** with thymine and adenine derivatives can be achieved by reacting the appropriate nucleobase acetic acid derivative $\mathbf{2B^p}$, prepared using slightly modified literature procedures,[31] with the telechelic macromonomer **1** using mixed anhydride peptide coupling conditions.[32] With the use of this methodology both the N^6-(4-methoxybenzoyl)adenine $\mathbf{A^{An}3A^{An}}$ and the N^4-(4-*tert*-butylbenzoyl)cytosine $\mathbf{C^{Pbz}3C^{Pbz}}$ could be prepared (Scheme 1) on a gram scale after purification by precipitation and column chromatography. ^{1}H NMR analysis of $\mathbf{A^{An}3A^{An}}$ and $\mathbf{C^{Pbz}3C^{Pbz}}$ (Figure 2) in DMSO-d_6 allows easy identification of peaks corresponding to the end groups and as such allows the calculation of the molecular weights (M_n) of these macromono-

(17) Lillya, C. P.; Baker, R. J.; Hütte, S.; Winter, H. H.; Lin, Y.-G.; Shi, J.; Dickinson, C.; Chien, J. C. W. *Macromolecules* **1992**, *25*, 2076−2080.
(18) Duweltz, D.; Lauprêtre, F.; Abed, S.; Bouteiller, L.; Boileau, S. *Polymer* **2003**, *44*, 2295−2302.
(19) For other examples of adenine and/or thymine derivatives attached to the ends of a core unit, see: (a) Higley, M. N.; Pollino, J. M.; Hollembeak, E.; Weck, M. *Chem. Eur. J.* **2005**, *11*, 2946−2953. (b) Binder, W. H.; Kunz, M. J.; Kluger, C.; Hayn, G.; Saf, R. *Macromolecules* **2004**, *37*, 1749−1759. (c) Binder, W. H.; Kunz, M. J.; Ingolic, E. *J. Polym. Sci., Part A: Polym. Chem.*, **2003**, *42*, 162. (d) Thibault, R. J.; Hotchkiss, P. J.; Gray, M.; Rotello, V. M. *J. Am. Chem. Soc.* **2003**, *125*, 11249. (e) Itahara, T. *Bull. Chem. Soc. Jpn.* **2002**, *75*, 285−290. (f) Iwaura, R.; Yoshida, K.; Masuda, M.; Yase, K.; Shimizu, T. *Chem. Mater.* **2002**, *14*, 3047−3053. (g) Shimizu, T.; Iwaura, R.; Masuda, M.; Hanada, T.; Yase, K. *J. Am. Chem. Soc.* **2001**, *123*, 5947−5955.
(20) Sivakova, S.; Rowan, S. J. *Chem. Soc. Rev.* **2005**, 9−21.
(21) Sartorius, J.; Schneider, H.-J. *Chem. Eur. J.* **1996**, *2*, 1446 and references therein.
(22) (a) Kersey, F. R.; Lee, G.; Marszalek, P.; Craig, S. L. *J. Am. Chem. Soc.* **2004**, *126*, 3038−3039. (b) Xu, J.; Fogleman, E. A.; Craig, S. L. *Macromolecules* **2004**, *37*, 1863−1870. (c) Fogleman, E. A.; Yount, W. C.; Xu, J.; Craig, S. L. *Angew. Chem., Int. Ed.* **2002**, *41*, 4026−4028. (d) Waybright, S. M.; Singleton, C. P.; Wachter, K.; Murphy, C. J.; Bunz, U. H. F. *J. Am. Chem. Soc.* **2001**, *123*, 1828−1833.
(23) (a) Giorgi, T.; Grepioni, F.; Manet, I.; Mariani, P.; Masiero, S.; Mezzina, E.; Pieraccini, S.; Saturni, L.; Spada, G. P.; Gottarelli, G. *Chem. Eur. J.* **2002**, *8*, 2143−2152. (b) Gottarelli, G.; Masiero, S.; Mezzina, E.; Spada, G. P.; Mariani, P.; Recanatini, M. *Helv. Chim. Acta* **1998**, *81*, 2078.
(24) (a) Takasawa, T.; Yoshikawa, I.; Araki, K. *Org. Biomol. Chem.* **2004**, *2*, 1125−1132. (b) Yoshikawa, I.; Li, J.; Sakata, Y.; Araki, K. *Angew. Chem., Int. Ed.* **2004**, *38*, 100−103.
(25) Förster, S.; Plantenberg, T. *Angew. Chem., Int. Ed.* **2002**, *41*, 688−714.
(26) Balsamo, V.; v. Gyldenfeldt, F.; Stadler, R. *Macromol. Chem. Phys.* **1996**, *197*, 3317−3341.
(27) de Lucca Freitas, L.; Jacobi, M. M.; Gonçalves, G. *Macromolecules* **1998**, *31*, 3379−3382.
(28) Abed, S.; Boileau, S.; Bouteiller, L. *Macromolecules* **2000**, *33*, 8479−8487.
(29) Öjelund, K.; Loontjens, T.; Steeman, P.; Palmans, A.; Maurer, F. *Macromol. Chem. Phys.* **2003**, *204*, 52−60.
(30) (a) Sivakova, S.; Rowan, S. J. *Chem. Commun.* **2003**, 2428−2429. (b) Sivakova, S.; Wu, J.; Campo, C. J.; Mather, P. T.; Rowan, S. J. *Chem. Eur. J.*, in press.
(31) Uhlmann, E.; Will, D. W.; Breipohl, G.; Langner, D.; Knolle, J. *Tetrahedron* **1995**, *51*, 12069−12082.
(32) Rowan, S. J.; Suwanmala, P.; Sivakova, S. *J. Polym. Sci., Part A: Polym. Chem.* **2003**, *41*, 3589−3596.

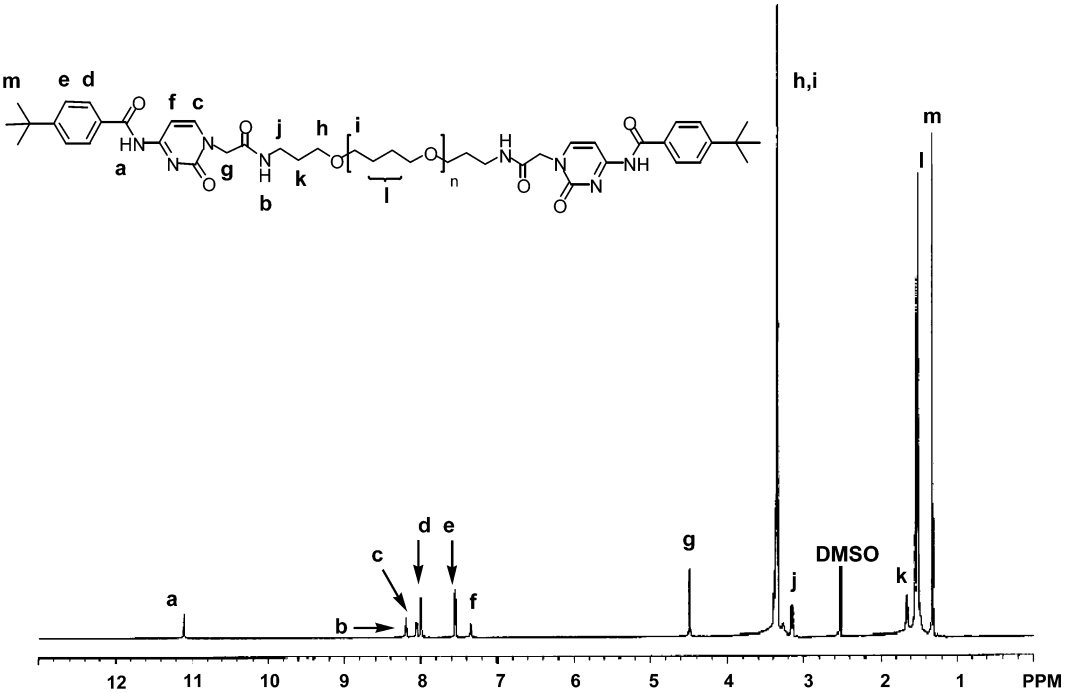

Figure 2. ^{1}H NMR (600 MHz) spectrum of N^4-(4-*tert*-butylbenzoyl)cytosine end-capped poly(tetrahydrofuran) (**C^{Pbz}3C^{Pbz}**) in DMSO-d_6 at room temperature.

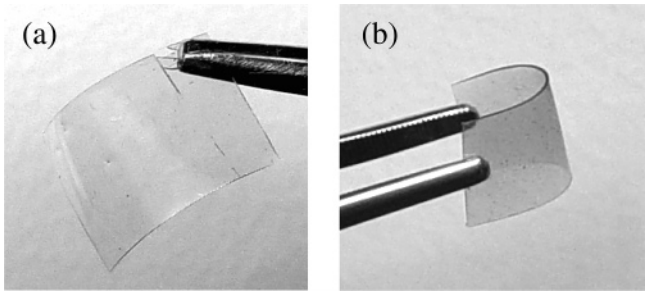

Figure 3. Pictures of the films formed from (a) **A^{An}3A^{An}** and (b) **C^{Pbz}3C^{Pbz}**.

mers to be ca. 1400 and 1650 g mol^{-1}, respectively. The M_n and polydispersity can also be estimated by MALDI-MS for both **A^{An}3A^{An}** (M_n = 1700 g mol^{-1}, PDI 1.14) and **C^{Pbz}3C^{Pbz}** (M_n = 1800 g mol^{-1}, PDI 1.18). The MALDI-MS also confirms the absence of any monosubstituted species in either of these materials.

While the amine-terminated poly(THF) **1** is a soft waxy material with a melting point of around 20 °C, the placement of the nucleobase derivatives on to the ends of **1** results in a marked change in the thermal and mechanical properties of the material. Specifically, an increase of over 100 °C in the melting point is observed upon such a derivatization: **A^{An}3A^{An}** exhibits a T_m of 135 °C while **C^{Pbz}3C^{Pbz}** exhibits a T_m of 126 °C on first heating. In addition, both these systems can be melt-processed into self-supporting films (Figure 3) and fibers. This is an interesting observation as the homoaggregation constant of both the cytosine and the adenine derivatives is not expected to be large. NMR dilution studies of the two protected nucleobase units using the model compounds N^6-(4-methoxybenzoyl)-9-(dodecyl)adenine (**C$_{12}$H$_{25}$A^{An}**) and 1-(methoxycarbonylmethyl)-N^4-(4-*tert*-butylbenzoyl)cytosine (**MeO$_2$CCH$_2$C^{Pbz}**) were used to estimate the K_a of these motifs to be ca. 1.5 ± 1 M^{-1} and 5 ± 2 M^{-1}, respectively, in $CDCl_3$. These values alone are not large enough to significantly enhance the mechanical properties of these systems, suggesting that other factors are playing an important role.

The nature of the end group is critical in determining the material properties of these systems. We have previously shown[33] that the placement of a large aromatic group that contains no hydrogen-bonding donor sites, 2,6-bis(1′-methylbenzimidazolyl)pyridine (Mebip), onto the end of the poly(THF) chain (**Mebip3Mebip**, Scheme 1) results in an oily material at room temperature. Thus, while a more exhaustive study still needs to be done, this initial work does suggest that hydrogen bonding does aid the formation of films in these systems. However, it should be noted that hydrogen bonding by itself is not enough. For example, we have shown that placement of a thymine moiety, which has a K_a similar to that of the protected adenine and cytosine derivatives (3.5 M^{-1} in $CDCl_3$),[21] onto the poly(THF) chain ends (**T3T**) results in a high melting point solid that shows no ability to form mechanically stable films.[32] This suggests, as one may expect, that there is a complex relationship between the supramolecular assembly of the end group, phase segregation, and crystallinity in these systems and that the right combination of these effects is required in order yield polymeric material properties from these otherwise low molecular weight monomers.

Furthermore, while the mechanical properties of the **C^{Pbz}3C^{Pbz}** and **A^{An}3A^{An}** macromonomers allow self-supporting films to be obtained, these materials do behave very differently from each other. The films of **C^{Pbz}3C^{Pbz}** (Figure 3b) are flexible, while the films of **A^{An}3A^{An}** are of a more brittle nature (Figure 3a) and easily developed cracks under stress. Thus, the main goal of this study was to obtain a better understanding of how and why the adenine- and cytosine-derived macromonomers form polymeric-like films and gain further insight into how the two nucleobase derivatives control the macromolecular assembly and, therefore, the resulting mechanical properties.

(33) Beck, J. B.; Ineman, J. M.; Rowan, S. J. *Macromolecules* **2005**, *38*, 5060−5068.

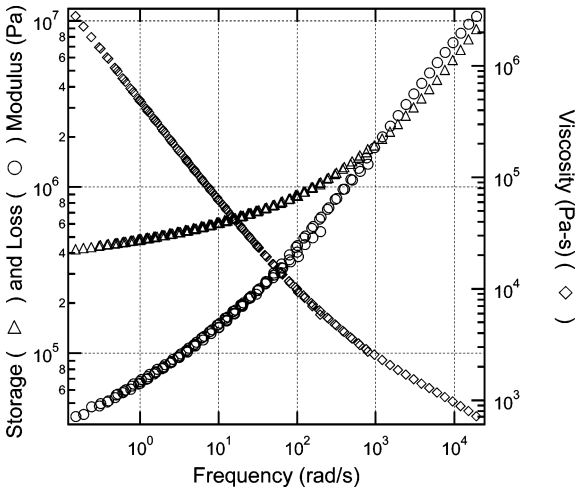

Figure 4. Low-temperature rheological behavior of $\mathbf{A^{An}3A^{An}}$ shifted to 50 °C. The rheological behavior is similar to that of a high molecular weight polymer. The modulus at low frequency and lack of a terminal viscosity suggest an extremely long relaxation time.

Thermal, Mechanical, and Structural Studies of the Adenine End-Capped Macromonomer ($\mathbf{A^{An}3A^{An}}$). The DSC thermograms for the $\mathbf{A^{An}3A^{An}}$ macromonomer show three endotherms at 86, 108, and 135 °C on the first heating. Further cooling and heating cycles of $\mathbf{A^{An}3A^{An}}$ reveal a small T_g-like transition at ca. 22 °C and reduced melting endotherms at 108 and 135 °C. Films of $\mathbf{A^{An}3A^{An}}$ can be prepared by simply heating the semicrystalline powder, originally obtained from a methanol precipitation, above its melting point (135 °C). Upon cooling, an optically clear film is obtained which shows endothermic transitions by DSC similar to those seen on the second heating of the semicrystalline powder. The enhancement of mechanical stability allows film formation consistent with the fact that this macromonomer self-assembles into higher molecular weight supramolecular structures. If supramolecular polymers are formed in the solid state then the material properties of these compounds would be expected to be sensitive to temperature. A rise in temperature should result in a weakening of the noncovalent interactions holding the polymer together, leading to a subsequent deaggregation of the monomer (repeat) units. While $\mathbf{A^{An}3A^{An}}$ melts at 135 °C upon the first heating, the material does not solidify upon cooling until ca. 100 °C. Above this lower limit fibers could be pulled from the melt until a temperature of ca. 130 °C is reached, at which point the viscosity of the material visually dropped and fibers could no longer be obtained. To further quantify this unusual melt behavior and to better understand the nature of the self-assembly in the solid state, a series of rheological studies was conducted.

The rheological study of $\mathbf{A^{An}3A^{An}}$ reveals a complex behavior. In the lower temperature range (50−90 °C) the material behaves in a thermorheologically simple manner, readily complying with time−temperature superposition,[34] as seen in Figure 4. The material exhibits behavior similar to that of either a high molecular weight polymer near the glass transition temperature or possibly a structured material.

Although the low-frequency terminal region has not been observed, an upper limit can be assigned to the material's relaxation time[35] which exceeds 10^3 s, indicative of extensive intermolecular associations and a material that behaves as a polymer of very high molecular weight, consistent with the findings of Gourier et al.[36] The plateau modulus in the low-temperature region (∼0.4 MPa) is close to, albeit slightly higher than, the estimate of 0.1 MPa from the model of Everaers et al.,[37] suggesting that the poly(THF) midblock is slightly stretched due to the end-to-end association or that the modulus is not wholly determined by the polymer block.

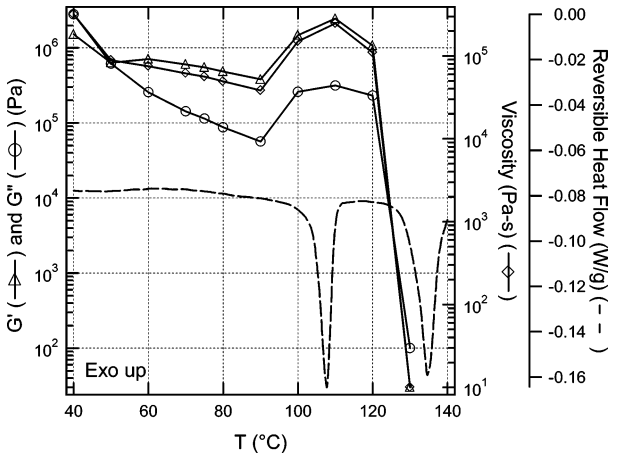

Figure 5. Temperature dependence of the rheological properties and thermal behavior of $\mathbf{A^{An}3A^{An}}$. The rheological properties of the material exhibit transitions that coincide with endothermic processes observed through MDSC.

At higher temperatures (100−120 °C) $\mathbf{A^{An}3A^{An}}$ exhibits behavior characteristic of a gel (network) at its critical point, namely, the storage modulus (G') is parallel to the loss modulus (G'') with respect to frequency (ω) on log−log coordinates. The transition to a gel phase is supported by an observed endothermic process in the modulated differential scanning calorimetry (MDSC) trace (Figure 5). Above this narrow gel temperature drastic decreases in the moduli and viscosity are observed, which coincide with a second endothermic process as observed in the MDSC trace.

The unusual rheological and thermal properties can be better understood by variable temperature FT-IR and WAXD characterization. Analysis of the FT-IR results (Figure 6) show N−H and C═O are involved in hydrogen bonding and that there is a rearrangement of this bonding between 70 and 90 °C in accord with the rheological measurements. At 35 °C the N−H stretching region (Figure 6a) shows a number of broad absorption bands in the 3200−3500 cm^{-1} region. Vibrations at 3455 cm^{-1} correspond to unbound N−H stretching, while the N−H peaks at 3371 and 3298 cm^{-1} are frequencies generally observed for medium strength hydrogen-bonded N−Hs.[38,39] This data implies that, in the solid state, $\mathbf{A^{An}3A^{An}}$ does indeed form some sort of hydrogen-bonded aggregate.

Upon heating from 70 to 90 °C the free N−H stretching vibration at 3455 cm^{-1} disappears and a new peak at 3415 cm^{-1} emerges. In addition, the two bound N−H stretching peaks at 3371 and 3298 cm^{-1} merge into a new broader peak centered

(34) Ferry, J. D. *Viscoelastic Properties of Polymers*, 3rd ed.; J. Wiley & Sons: New York, 1980.
(35) Graessley, W. W. *Adv. Polym. Sci.* **1974**, *16*, 1−179.
(36) Gourier, C.; Rincet, F.; Le Bouar, T.; Zhang, Y.; Esnault, J.; Mallet, J.-M.; Sinay, P.; Perez, E. *Macromolecules* **2004**, *37*, 8778−8784.
(37) Everaers, R.; Sukumaran, S. K.; Grest, G. S.; Svaneborg, C.; Sivasubramanian, A.; Kremer, K. *Science* **2004**, *303*, 823−826.
(38) Lee, J. Y.; Painter, P. C.; Coleman, M. M. *Macromolecules* **1988**, *21*, 954.
(39) Lambert, J. B.; Shurvell, H. F.; Lightner D. A.; Cooks, R. G. *Organic Structural Spectroscopy*; Prentice Hall: Upper Saddle River, NJ, 1998.

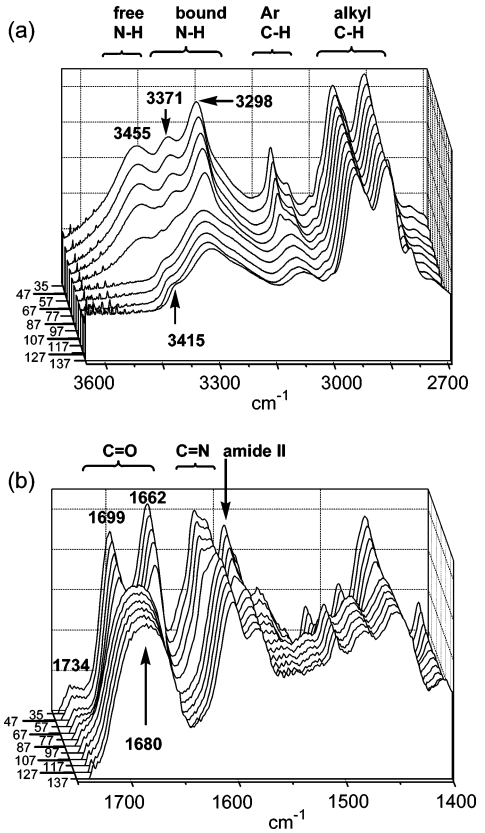

Figure 6. Variable temperature FT-IR spectra in the (a) 2700−3600 cm^{-1} region and (b) 1400−1750 cm^{-1} region of N^6-(4-methoxybenzoyl)adenine-terminated poly(tetrahydrofuran) ($\mathbf{A^{An}3A^{An}}$) (film, CaF_2 disk).

at 3311 cm^{-1}. In the lower region (1400−1750 cm^{-1}) of the FT-IR spectra (Figure 6b) we observe three carbonyl stretching peaks in the sample at 35 °C: a weak peak at 1734 cm^{-1}, consistent with non-hydrogen-bonded carbonyls, and two much stronger peaks 1699 and 1662 cm^{-1}, which have been tentatively associated[19g] with the aromatic protecting group carbonyl stretch and the aliphatic carbonyl stretch. The carbonyl stretching region also shows a transition between 70 and 90 °C. In this case, the two major carbonyl peaks, at 1699 cm^{-1} and 1662 cm^{-1}, merge into one much broader peak centered at 1680 cm^{-1}, suggestive of a change in the nature of the hydrogen bonding at that temperature.

Taken together these results are consistent with the idea that formation of a more extensively cross-linked material occurs as a consequence of an increase in amide hydrogen bonding. Presumably at lower temperatures some of the end groups have been "frozen" in a non-hydrogen-bonding state. However, upon reaching 70 °C there is enough thermal energy in the system for these moieties to rearrange, allowing the end groups' hydrogen bonding to be maximized. It should be noted though that while there is loss of mechanical properties of the film above 130 °C this does not appear to be a consequence of significant dissociation of hydrogen bonds as no free N−H stretching peak is observed even at 150 °C. It is more probable that above 130 °C there is a significant reduction in phase segregation as the end groups start to become soluble in the poly(THF) matrix.

To further understand the structural nature of the $\mathbf{A^{An}3A^{An}}$ macromonomer, wide-angle X-ray diffraction studies (WAXD) were performed on the annealed film sample. With the use of WAXD (Cu Kα: $\lambda = 1.54$ Å), the diffraction pattern of the

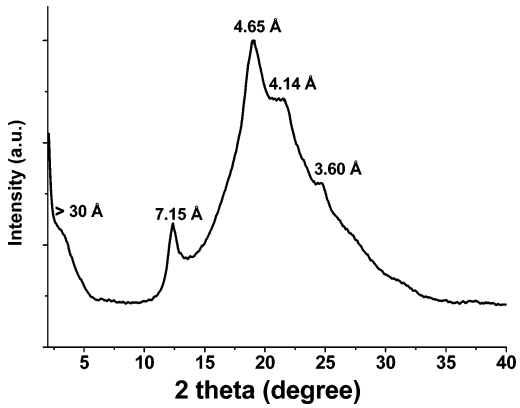

Figure 7. X-ray (radiation source Cu Kα) diffraction diagram of the $\mathbf{A^{An}3A^{An}}$ film at room temperature.

$\mathbf{A^{An}3A^{An}}$ film (Figure 7) displays a number of reflection peaks at $2\theta = 12.31°$ ($d = 7.15$ Å), 19.03° ($d = 4.65$ Å), 21.44° ($d = 4.14$ Å), 24.54° ($d = 3.60$ Å), 30.5° ($d = 2.93$ Å), and 31.5° ($d = 2.84$ Å).

The reflection peak corresponding to d spacing of 3.60 Å is consistent with the presence of $\pi-\pi$ stacking between the nucleobases within the "hard" phase. Furthermore, the reflection peak at $2\theta = 12.31°$ ($d = 7.15$ Å) suggests that within these "hard" domains there are stacks of the nucleobase which are held together with $\pi-\pi$ interactions and, from the FT-IR data, amide hydrogen bonding. To further investigate the effects of temperature on this material, variable temperature X-ray experiments were carried out (see the Supporting Information). At 70 °C, both reflections that correspond to d spacings of ca. 7.15 and 3.60 Å have disappeared, implying that by this temperature a significant reduction in the amount of $\pi-\pi$ stacking has occurred. This is consistent with an increase in the molecular motion of the hard segment, which results in an increase in hydrogen bonding and subsequent conversion to a gel.

In the event of phase segregation in the $\mathbf{A^{An}3A^{An}}$ system, we would anticipate a reflection which represents the spacing between the hard segments. In fact, we observe a shoulder in the WAXD data at lower angles which corresponds with a d spacing of >30 Å (Figure 7). Further experiments using a Si (111) double-crystal monochromator (see the Supporting Information) showed that the reflection corresponds to a d spacing of ca. 39.8 Å. In addition, the WAXD data show that the material has a degree of crystallinity, calculated using Ruland's method,[40] of ca. 14.2%.

All these results point to a model given in Figure 8 where at lower temperature there is a phase-segregated material in which some of the chain ends are not hydrogen bonded, and as such, the material behaves like a high molecular weight linear polymer. In this model relatively long "hard" semicrystalline stacks of the adenine chain ends form within the "soft" poly(THF) matrix. Some of the adenine chain ends are frozen in non-hydrogen-bonding modes, while others are interacting with each other joining together adjacent stacks. The concentration of such stacks is below the percolation threshold, and as such, the material behaves more like a linear rather than a cross-linked network.

The plateau modulus, G_0, of the material can be related to M_e, the average molecular weight between entanglements or cross-links. Assuming the density of the material is ap-

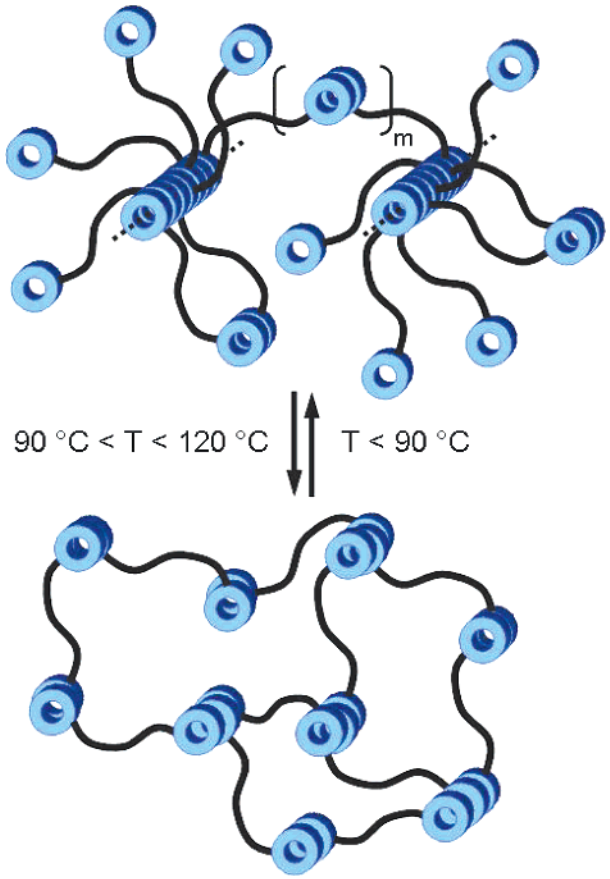

Figure 8. Schematic model of the proposed $\mathbf{A^{An}3A^{An}}$ assembly as it transitions at 90 °C from a linear system to a gellike material. The schematic shows the segregation of the nucleobase hard segments (disks) connected by chains of poly(THF)s (lines).

proximately similar to that of the starting poly(THF) **1** then M_e can be estimated to be approximately 8000 g mol^{-1}. If the main cross-links occur at the stacks then this would correspond approximately to the aggregation (m) of 5−6 chains of $\mathbf{A^{An}3A^{An}}$ between stacks. This distance is consistent with the ca. 4 nm d spacing observed in the WAXD data mentioned above. Between 70 and 90 °C there is a change in the hard segment bonding, and a thermal rearrangement occurs, resulting in a decrease in $\pi-\pi$ stacking between the nucleobases but an effective increase in hydrogen bonding. This corresponds to a change in the mechanical behavior of the material suggesting a conversion from a linear polymer to a gellike cross-linked architecture above 90 °C (Figure 8). In this model the large stacks have broken up into a larger number of smaller more disordered stacks. The concentration of these smaller stacks is now above the percolation threshold, and the system behaves like a gel. Further increase in temperature (>130 °C) yields a material which shows little or no polymer-like properties. However, there still appears to be a significant amount of hydrogen bonding present in this system. Thus a possible explanation for the significant reduction in mechanical properties is that above ca. 130 °C an order−disorder transition occurs, and as such, a reduction in phase segregation results.

Thermal, Mechanical, and Structural Studies of the Cytosine End-Capped Macromonomer ($\mathbf{C^{Pbz}3C^{Pbz}}$). The N^4-(4-*tert*-butylbenzoyl)cytosine end-capped poly(tetrahydrofuran) ($\mathbf{C^{Pbz}3C^{Pbz}}$) macromonomer shows an increase in its melting temperature by 88 °C on the first heating compared to that of

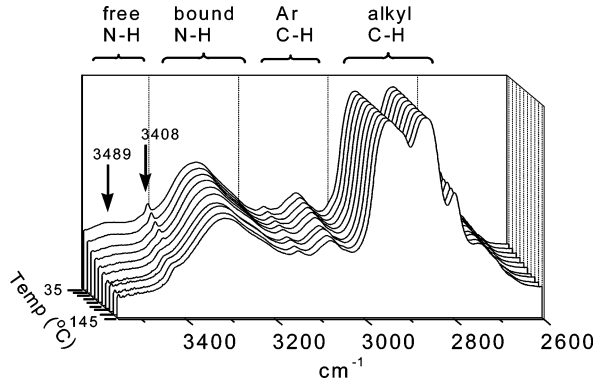

Figure 9. Variable temperature FT-IR spectra of N^4-(4-*tert*-butylbenzoyl)-cytosine-terminated poly(tetrahydrofuran) ($\mathbf{C^{Pbz}3C^{Pbz}}$) (film, CaF_2 disk). Spectra were taken at 35, 45, 55, 65, 75, 85, 95, 105, 135, and 145 °C. Arrows indicate the N−H vibrations which diminish with increasing temperature.

the underivatized amine-terminated poly(tetrahydrofuran) (**1**). As mentioned before, like $\mathbf{A^{An}3A^{An}}$, both films and fibers of $\mathbf{C^{Pbz}3C^{Pbz}}$ can be obtained by melt processing. However, the films of $\mathbf{C^{Pbz}3C^{Pbz}}$ appear tougher and more flexible than the $\mathbf{A^{An}3A^{An}}$ films.

FT-IR (Figure 9) and WAXD experiments were carried out to investigate the nature of the noncovalent interactions present in $\mathbf{C^{Pbz}3C^{Pbz}}$. Like $\mathbf{A^{An}3A^{An}}$, the room-temperature FT-IR spectrum of this material shows a number of broad absorption bands in the 3200−3500 cm^{-1} region. The most apparent difference between the materials' spectra is seen in the intensity of the unassociated N−H peak which is much smaller in $\mathbf{C^{Pbz}3C^{Pbz}}$ than $\mathbf{A^{An}3A^{An}}$. This observation suggests the formation of a network in the cytosine material at room temperature. However, like the $\mathbf{A^{An}3A^{An}}$ material, a decrease in the intensity of the free N−H stretch is observed with increasing temperature, suggesting that there is again an increase in the amount of hydrogen bonding with increasing temperature. The decrease in intensity of these vibrations was much more gradual in contrast to the sharp changes in the free and associated N−H stretching intensities observed for $\mathbf{A^{An}3A^{An}}$ at approximately 90 °C.

The WAXD data (see the Supporting Information) of the annealed (>140 °C) sample shows only one broad reflection at $2\theta = 18.4°$ ($d = 4.67$ Å), so, unlike $\mathbf{A^{An}3A^{An}}$, within the "hard" nucleobase domains of $\mathbf{C^{Pbz}3C^{Pbz}}$ there is no regular $\pi-\pi$ stacking. This is perhaps not surprising considering the reduced π-surface of the cytosine compared to that of the adenine and the presence of the bulky *tert*-butyl moiety on the aromatic protecting group of the cytosine. Further experiments, using a Si (111) double-crystal monochromator (see the Supporting Information), showed that a low-angle reflection corresponding to a d spacing of 46.2 Å was observed, consistent with the formation of phase segregation. It should be noted that this reflection appears more diffuse than the low-angle reflection observed for the $\mathbf{A^{An}3A^{An}}$ which may suggest that there is a weaker segregation limit in the cytosine end-capped material. In addition, the data suggest that the material has a much lower degree of crystallinity[40] (6.3%) than the adenine end-capped material (14.2%).

To investigate the nature of this material further and allow comparison between the two nucleobase end-capped mac-

(40) Alexander, L. E. *X-ray Diffraction Methods in Polymer Science*; John Wiley and Sons: London, 1969.

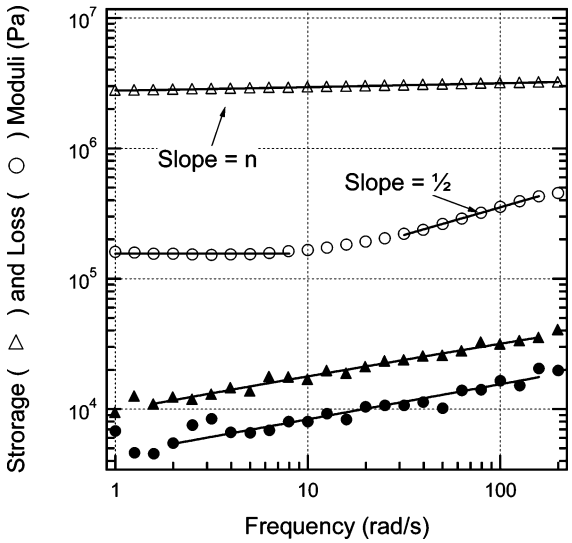

Figure 10. Shear moduli as a function of frequency for $\mathbf{C^{Pbz}3C^{Pbz}}$ at 90 °C (open symbols) and 120 °C (filled symbols). A power law is apparent at all temperatures for both the storage (G') and loss (G'') modulus. At low temperature and high frequency, the loss modulus showed an increase due to the excitation of Rouse motions. The power law relation for G' is used to determine the rheological strength (S) and relaxation exponent (n). Note: At lower temperatures (open symbols), the loss modulus is seen to increase at higher frequencies. It is believed that this is due to extra dissipation at length scales smaller than that of the network dimensions, i.e., Rouse time scales are excited demonstrating a power law of $^1/_2$. This effect is expected (ref 45) and is not critical to any major conclusion.

romonomers, rheological studies, similar to the one previously discussed for $\mathbf{A^{An}3A^{An}}$, were performed on $\mathbf{C^{Pbz}3C^{Pbz}}$. Unlike $\mathbf{A^{An}3A^{An}}$, the $\mathbf{C^{Pbz}3C^{Pbz}}$ material behaved like a critical gel (or network) at all temperatures with the material loss factor ($\tan(\delta) \equiv G''/G'$) independent of frequency except at high frequency and low temperature (Figure 10). The gel-type behavior lent itself to analysis with the gel model developed by Winter and co-workers:[41,42]

$$G' = \frac{\pi S \omega^n}{2\Gamma(n)\sin(n\pi/2)} = \frac{G''}{\tan(n\pi/2)} \qquad (1)$$

where S is a network strength and n a relaxation exponent. Fitting eq 1 to the data allowed determination of a fractal-like strength parameter, S, and relaxation exponent, n, at each measured temperature to grade the material strength according to the method proposed by Scanlan and Winter[43] and effectively utilized by Halley and Mackay.[44]

From dimensional analysis, it is expected that $S = G_0 t_0^n$ where G_0 is a material modulus and t_0 a time scale. Thus, a plot of $\log(S)$ versus n, as seen in Figure 11, allowed the determination of the inherent modulus and time scale. This data shows an interesting transition occurs in the material at around 105 °C. While there appears to be no change in the material modulus, a significant difference was observed in the calculated time scale.

Previous work has implied that G_0 is akin to the plateau modulus (G_N^0) for the polymeric strands. Estimation of the plateau modulus for the poly(THF) inner block was performed through the relation given by Everaers et al.,[37] as discussed

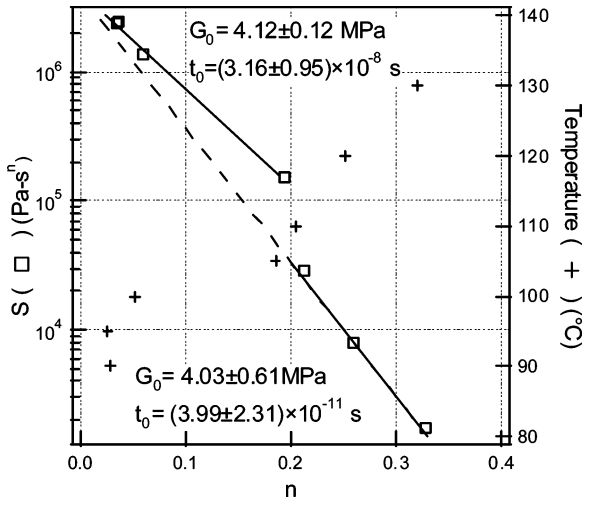

Figure 11. Rheological strength as a function of power law for $\mathbf{C^{Pbz}3C^{Pbz}}$. There is a distinct break in the relation for temperature greater than 105 °C yielding two values for the material modulus (G_0) and time scale (t_0) determined from the relation $S = G_0 t_0^n$.

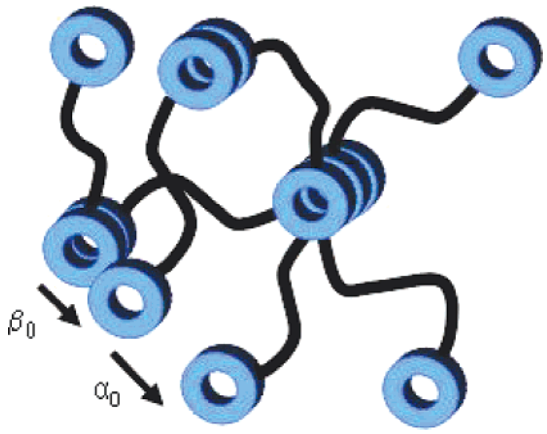

Figure 12. Schematic of the network of telechelic polymers. Hopping between the nucleobase (disk) rich regions is determined by the association (α_0) and dissociation (β_0.) frequencies.

above, to yield a value of ~0.1 MPa. The value of G_0 (~4 MPa) shown in Figure 11 is clearly larger and so must be produced by another mechanism.

To understand the behavior of this material in more detail we employed the model developed by Vaccaro and Marrucci[46] to describe the rheological properties of associating polymers in solution (Figure 12). It is assumed in this model that there is a network formed by phase-segregated chain ends held together by a soluble chain, where the chain ends can hop between the phase-segregated regions. The plateau modulus (eq 2) in such a network depends on the fraction of pendent chains (y_p), in which one chain end is not incorporated into the network, and active chains (y_a), in which both chain ends are incorporated into the network.

$$G_N^0 = \nu k_B T[y_a/\tau\beta_0 + y_p\tau\beta_0] \qquad (2)$$

where ν is the number of chains per unit volume and k_B and T are Boltzmann's constant and temperature, respectively. The τ

(41) Vallés, E. M.; Carella, J. M.; Winter, H. H.; Baumgaertel, M. *Rheol. Acta* **1990**, *29*, 535−542.
(42) Winter, H. H. *Polym. Eng. Sci.* **1987**, *27*, 1698−1702.
(43) Scanlan, J. C.; Winter, H. H. *Macromolecules* **1991**, *24*, 47−54.
(44) Halley, P. J.; Mackay, M. E. *Polymer* **1994**, *35*, 2189−2191.
(45) Hahn, H.; Lee, J. H.; Balsara, P. N.; Garetz, B. A.; Watanabe, H. *Macromolecules* **2001**, *34*, 8701−8709.
(46) Vaccaro, A.; Marrucci, G. *J. Non-Newtononian Fluid Mech.* **2000**, *92*, 261−273.

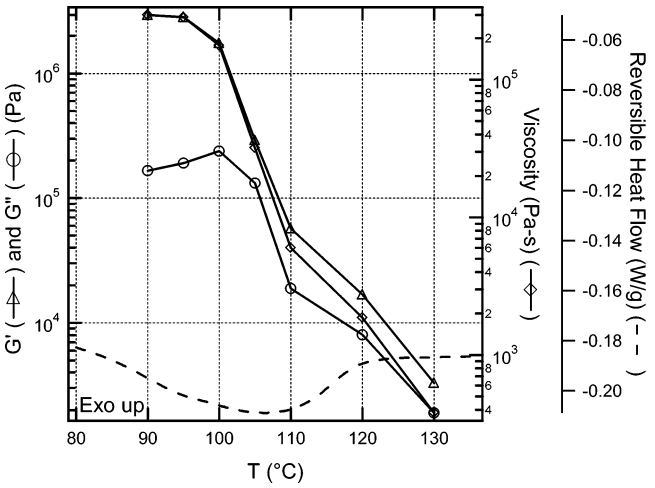

Figure 13. Temperature dependence of the rheological properties and thermal behavior of $\mathbf{C^{Pbz}3C^{Pbz}}$. The rheological properties of $\mathbf{C^{Pbz}3C^{Pbz}}$ measured at 10 rad s^{-1} exhibit a transition that coincides with the shifts in t_0. This transition is corroborated by a broad endothermic process observed via MDSC.

term represents the relaxation time for the chain if it did not participate in the network at all.

The fraction of active and pendent chains depends on the disengagement rate from the network, β_0, as well as the attachment rate to the network, α_0. The infrared absorption data of $\mathbf{C^{Pbz}3C^{Pbz}}$ suggests there are few pendent chains, and therefore the modulus we measure is assumedly related to $\nu k_B T/\tau\beta_0(y_a \rightarrow 1, y_p \rightarrow 0)$. Clearly, the dilute solution Vaccaro−Marrucci model is not strictly applicable to our concentrated, dense system; yet, eq 2 suggests that the relaxation time gleaned from the fractal analysis shown in Figure 11 has a relaxation time scaled with a detachment frequency. This may explain why the time scales, t_0, are so small and that at a certain temperature, 105 °C, the disengagement rate from the network can cause an abrupt change in the rheological properties without affecting the modulus ($\sim\nu k_B T$) we determine with the fractal analysis. Further, the fraction of pendent chains ($y_p = \beta_0/[\alpha_0 + \beta_0]$) need not significantly increase when the change occurs in the limit of large attachment rate ($\alpha_0 \gg \beta_0$), and so the rheological properties can be dominated by the disengagement rate and its direct influence on the modulus. This is an interesting result as it suggests that increasing the rate of disengagement, for example, by increasing the rate of decomplexation, should result in significant changes in the rheological properties in such a film. Finally, the modulus magnitude appears to be correctly predicted by the number of polymer molecules per unit volume (ν) since $\nu k_B T$ is found equal to 2 MPa in good agreement with the value found with the fractal analysis.

Predictably, the temperature at which t_0 changes (105 °C) corresponds to the temperature at which the viscosity decreases (Figure 13). The moduli and viscosity in the low-temperature regime show relatively little change with temperature. However, near the transition point in relaxation time, 105 °C, a stark shift in that trend occurs with a drop of over a decade in each property.

Characterization by MDSC supports the observation of a transition by showing an endothermic peak at 107 °C (Figure 13) which can be attributed to a shift in the type of intermolecular forces that govern network formation in each regime. With this in mind, it becomes clear that the gel−gel transition may be controlled by not only the strength of interactions between end groups, the size and composition of the middle block, but also by the rate of dissociation of the chain end from the network.

Conclusion

We have demonstrated that polymer-like properties can be obtained with supramolecular materials that employ weak hydrogen bond interactions in conjunction with phase segregation. These materials appear to show a different responsive behavior than is observed for supramolecular polymers which utilize much stronger degrees of interaction. The data suggests that the rheology of these systems is strongly dependent on the end groups' dissociation frequency from the "hard" segments.[47] If this proves to be general then it becomes an important design parameter for the development of new highly thermally responsive materials. For example, the rate of decomplexation of the ends groups, T_g of the hard segment, and the compatibility of the hard and soft segments can all be tailored to alter this dissociation rate. We show that the rheological behavior of the telechelic polymers is strongly influenced by the end groups' chemistry. In the case of the cytosine end-capped material, a network (gel) structure is observed at room temperature. The gel model of Winter et al., which was originally developed to describe irreversibly cross-linked networks, is shown to be useful for the analysis of telechelic networks' reversible association. In addition, despite having a relatively similar overall structure to the cytosine end-capped material, the adenine end-capped material is seen to behave in a drastically different manner. Incomplete association is observed at lower temperatures with an eventual transition to a network at higher temperatures prior to a sharp transition to complete loss of polymer-like properties. The ability to easily tailor the molecular structure of the nucleobase (or other aromatic hydrogen-bonding) end groups, as well as the core, to alter the degree and nature of phase segregation and hydrogen bonding offers a very flexible platform for materials development. Work is continuing in this area to elucidate the structure/self-assembly/property relationships in this class of supramolecular polymers. The development of such materials, which exhibit very low melt viscosities, potentially allows access to a new range of thermally rehealable plastics as well as easy-to-process and/or recycle materials.

Experimental Section

Materials. 1-(Carboxymethyl)-N^4-(*tert*-butylbenzoyl)cytosine ($\mathbf{2C^{Pbz}}$) and the N^6-(4-methoxybenzoyl)adenine-terminated poly(tetrahydrofuran) ($\mathbf{A^{An}3A^{An}}$) were synthesized according to literature procedures.[32,48] All reagents and solvents were purchased from Aldrich Chemical Co. Reagents were used without further purification. Solvents were distilled from suitable drying agents.

Instruments. NMR spectra were recorded on a Varian Gemini 200 MHz NMR, a Varian 300 MHz, or a Varian 600 MHz spectrometer. Fourier transform infrared (FT-IR) measurements were performed on a Biorad Excalibur series FTS3000MX spectrometer. Molecular weights of materials were measured by mass spectrometry on a Bruker BIFLEX III matrix-assisted laser desorption/ionization time-of-flight mass spectrometer (MALDI-TOF-MS, matrix: α-cyano-4-hydroxycinnamic acid). Wide-angle variable tempearture X-ray data obtained on Rigaku

(47) Yount, W. C.; Loveless, D. M.; Craig, S. L. *J. Am. Chem. Soc.* **2005**, *127*, 14488−14496.
(48) David, W. W.; Gerhard, B.; Dietrich, L.; Jochen, K.; Eugen, U. *Tetrahedron* **1995**, *51*, 12069−12082.

RINT 2000/PC series diffractometer with a Rigaku programmable temperature controller PTC-30. Additional wide-angle X-ray data were collected at the Advanced Photon Source, Argonne National Laboratory (Chicago, IL) on the DND-CAT beamline 5. The samples were investigated in transmission mode. A Si (111) double-crystal monochromator was used, the crystals of which were detuned with respect to each other using a piezo crystal tilt stage to reduce the amount of harmonics in the Bragg-reflected beam. For these experiments, the monochromator was detuned to typically 80% of the maximum of the rocking curve. X-rays of 35 keV collimated to 1 mm diameter were used. Wide-angle X-ray patterns were collected using the CCD Mar 165 using typically 60 s exposure. The sample-to-detector distance was 782 mm, and this was calibrated using silver behenate. Data reduction and data analysis were performed using the Polar v 2.6 software package (Stonybrook Technology and Applied Research Inc.). Rheological testing, using a Rheometrics ARES controlled strain rheometer, was performed under dynamic shear with care taken to limit data gathered to within the linear viscoelastic range. The 8 mm parallel plate geometry was used to limit sample size to ca. 25 mg. The networks were extremely robust, and maximum shear strains less than 1% had to be used at all temperatures. Void-free samples were made under vacuum at temperatures in excess of 120 °C to ensure that neither air bubbles nor moisture influenced the results. Thermal analysis was conducted using a TA Instruments modulated differential scanning calorimeter (MDSC) model Q1000. Samples were tested using heat-only MDSC with an overall temperature ramp rate of 5 °C/min and a modulation period of 40 s. Samples were approximately 3 mg, and a nitrogen purge gas was used. The instrument was fully calibrated with indium and sapphire standards.

Synthesis of N^4-(4-*tert*-Butylbenzoyl)cytosine-Terminated Poly(tetrahydrofuran) ($\mathbf{C^{Pbz}3C^{Pbz}}$). 1-(carboxymethyl)-N^4-(4-*tert*-butylbenzoyl)cytosine (**2C^{Pbz}**) (0.6 g, 1.82 mmol) was dissolved in dry DMF (5 mL), and the solution was cooled to 0 °C. Trimethylacetyl chloride (0.17 mL, 1.38 mmol) was then added dropwise, and the reaction stirred for an addition 10 min, before *N*-methyl morpholine (0.38 mL, 3.45 mmol) was added dropwise, and the reaction stirred for another 1 h. To the stirring solution was added 0.50 g (0.45 mmol) of bis(3-aminopropyl)-terminated poly(tetrahydrofuran) (**1**) dissolved in 10 mL of dry DMF. The reaction was stirred for 48 h while warming to room temperature. The solvent was removed and the residue treated with EtOAc. The EtOAc fraction was then evaporated in a rotary evaporator. The resulting crude product was precipitated from mixture of water and methanol to give a white solid **C^{Pbz}3C^{Pbz}** in 0.52 g (66%) yield. The reaction was repeated three times to ensure complete reaction of the amino chain ends. ^{1}H NMR (600 MHz, DMSO-d_6): δ 11.10 (2H, s, cytosine NH), 8.20 (2H, s, NH), 8.06 (2H, d, J = 7.8 Hz, cytosine H-6), 8.00 (4H, d, J = 8.4 Hz, tBuBz H-2 and 6), 7.55 (4H, d, J = 7.8 Hz, tBuBz H-3 and 5), 7.34 (2H, d, J = 7.2 Hz, cytosine H-5), 4.48 (4H, s, cytosine CH_2), 3.34 (64H, m, CH_2), 2.56 (4H, m, CH_2), 1.61 (4H,m CH_2), 1.52 (60H, m, CH_2), 1.31 (18H, s, tBu); M_n = 1865 g mol^{-1}. ^{13}C NMR (50 MHz, DMSO-d_6): δ 26.22, 29.40, 30.94, 34.87, 36.12, 51.54, 69.85, 95.64, 125.33, 128.47, 130.51, 151.30, 155.79, 163.44, 166.50. IR (solid, KBr disk): 3416, 2945, 2854, 1662, 1556, 1490, 1363, 1254, 1115 cm^{-1}. IR (film, KBr disk): 3298, 2945, 2854, 1665, 1556, 1493, 1366, 1251, 1116 cm^{-1}. MALDI-MS (2-(4-hydroxyphenylazo) benzoic acid): M_n = 1833 g mol^{-1}, M_w = 2169 g mol^{-1}, PDI = 1.18. DSC (T_m = 126 °C).

Acknowledgment. Financial support from Michigan State University, the NIH (NIBIB: EB-001466-01), and the Case School of Engineering is gratefully acknowledged. The authors also thank Professor P. T. Mather (Case) and Dr. A. Romo-Uribe (Rohm & Haas) for help with some of the X-ray experiments.

Supporting Information Available: Synthetic procedures and characterization of **2A^{An}**, along with ^{1}H, ^{13}C NMR, MALDI-MS, FT-IR, and WAXD data of **A^{An}3A^{An}** and **C^{Pbz}3C^{Pbz}**. This material is available free of charge via the Internet at http://pubs/acs/org.

JA055245W